Mineralogy and Petrology (2006) 87: 187–207
DOI 10.1007/s00710-006-0130-z

Mineralogy and Petrology

Printed in Austria

Te and Se mineralogy of the high-sulfidation Kochbulak and Kairagach epithermal gold telluride deposits (Kurama Ridge, Middle Tien Shan, Uzbekistan)

O. Yu. Plotinskaya[1], **V. A. Kovalenker**[1], **R. Seltmann**[2], and **C. J. Stanley**[2]

[1] Institute of Geology of Ore Deposits, Petrography, Mineralogy, and Geochemistry (IGEM RAS), Moscow, Russia
[2] CERCAMS, Department Mineralogy, Natural History Museum, London, Great Britain

Received April 15, 2005; revised version accepted March 20, 2006
Published online June 14, 2006;
Editorial handling: P. Spry

Summary

The Late Paleozoic Kochbulak and Kairagach deposits are located on the northern slope of the Kurama Ridge, Middle Tien Shan, in the same volcanic structure and the same ore-forming system. Au–Ag–Cu–Bi–Te–Se mineralization is confined to veins and dissemination zones accompanied by quartz-sericite wall-rock alteration. The tellurides, calaverite, altaite, hessite, and tetradymite are widespread at both deposits; at Kairagach selenides and sulfoselenides of Bi and Pb are common, while at Kochbulak Bi and Pb telluroselenides and sulfotelluroselenides are typical. The paragenetic sequence of telluride assemblages are similar for both deposits and change from calaverite + altaite + native Au to sylvanite + Bi tellurides + native Te, Bi tellurides + native Au, and, finally, to Au + Ag tellurides with time. These mineralogical changes are accompanied by an increase in the Ag content of native gold that correlates with a decrease in temperature, fTe_2 and fO_2 and an increase in pH.

Introduction

Most volcanic-hosted epithermal gold deposits (*White* and *Hedenquist*, 1990; *Bonham*, 1986; *Heald* et al., 1987; *Henley*, 1991) are of Neogene or Paleogene age. However, some of the largest deposits, including Kochbulak, Uzbekistan, are Paleozoic in age. The Kochbulak and smaller Kairagach deposits are located 3.5 km apart near the town of Angren on the northern slope of the Kurama Ridge in the Middle Tien Shan. The Kurama Ridge forms the eastern part of the extensive Bel'tau-Kurama volcano-plutonic belt. Some modern geotectonic reconstructions of this belt (*Dalimov* and *Ganiev*, 1994; *Zonenshain* et al., 1990) consider it to have been an Andean-type continental margin volcanic belt that formed in the Late Paleozoic on a Precambrian and Early Hercynian continental basement. This belt is unusual in that it contains Paleozoic porphyry Au–Cu–Mo, Ag–Pb–Zn skarn and epithermal Au–Ag–Te–Se deposits (Fig. 1). The total gold resources of this region exceed 2000 tonnes (*Islamov* et al., 1999), which makes this region a world-class gold province. The estimated reserves of the Kochbulak deposit are 120 t of Au and 400 t of Ag. Major ore components are Au (13.4 ppm) and Ag (120 ppm), also Cu (0.2%), Se (4 ppm), Te (101.6 ppm) and Bi (0.01%). Reserves of the Kairagach deposit are relatively small and are estimated to be 50 t of Au and 150 t of Ag. Gold is present mostly in native form but approximately 20–25% of the total gold reserves of these two deposits occur as various precious metal tellurides. Some researchers suggest that the Kochbulak and Kairagach deposits are part of a single Kochbulak–Kairagach ore field (*Islamov* et al., 1999).

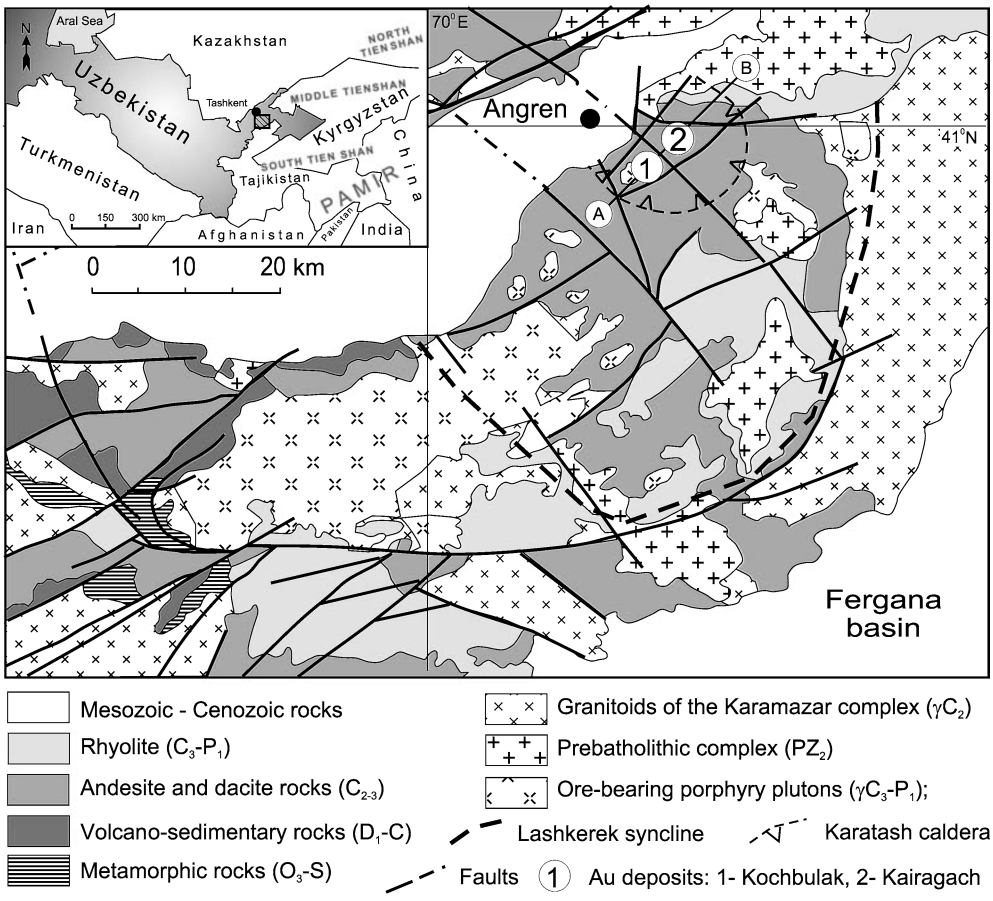

Fig. 1. Schematic geological map of the central part of the Kurama Ridge (after *Kovalenker* et al., 2003)

The geological, geochemical, and mineralogical features of the Kairagach and Kochbulak deposits have been described by a number of workers (*Genkin* et al., 1980; *Badalov* and *Spiridonov*, 1983; *Badalov* et al., 1984; *Spiridonov* and *Badalov*, 1983; *Kovalenker* and *Heinke*, 1984; *Kovalenker* et al., 1979, 1980, 1997, 2003; *Plotinskaya* and *Kovalenker*, 1998; *Koneev* and *Gertman*, 1997; *Plotinskaya* et al., 2001). However, no comparative mineralogical description of these deposits has been undertaken.

The objective of the present communication its to describe and to compare the telluride and selenide mineralogy of the Kochbulak and Kairagach deposits using both published and recently obtained mineral chemistry to refine the conditions of tellurides deposition at the both deposits.

Geological setting

The Kochbulak and Kairagach deposits occur in the Karatash (or Kochbulak–Kairagach) caldera in the northern part of the Lashkerek volcano-tectonic depression (Figs. 1 and 2) at the intersection of the South Angren and Lashkerek-Dukent fault zones (*Islamov* et al., 1999). The caldera is filled with volcano-sedimentary and subvolcanic rocks (>1.5 km thick) of andesite–dacite and rhyolite composition. The andesite–dacite unit (C_{2-3}) consists of andesitic and dacitic lavas, tuffs, and sandstones that were intruded by subvolcanic dacite–porphyry and diorite–porphyry stocks. The rhyolite unit (C_3-P_1) consists of rhyolitic lavas and pyroclastic rocks. Numerous north–east trending diabase porphyry and granodiorite porphyry dikes (C_3-P_1) occur throughout the Karatash caldera. In the central part of the caldera a stock-shaped subvolcanic intrusion of porphyritic trachyandesite (C_3-P_1), which is considered to be a volcanic neck, separates the Kochbulak and Kairagach ore fields (*Islamov* et al., 1999; *Kovalenker* et al., 1997, 2003). Volcanic rocks were affected by synvolcanic albite-chlorite and sericite-chlorite alteration.

Precious metal mineralization Kochbulak and Kairagach is confined to silicification and breccia zones accompanied by quartz-sericite wall-rock alteration. At Kochbulak, three types of ore bodies have been recognized: (1) pipe-like ore bodies,

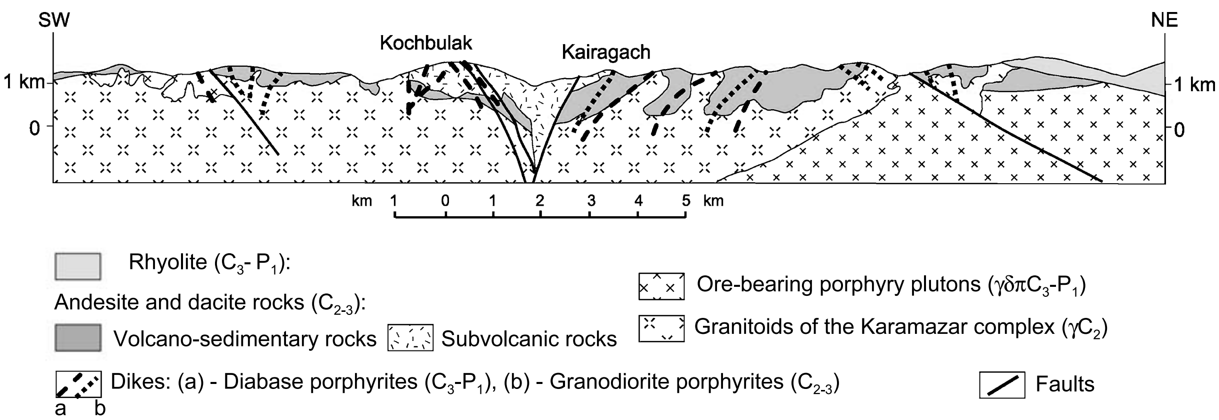

Fig. 2. Schematic cross-section through the Karatash caldera along the line A–B shown on Fig. 1

(2) flat (20–40°) lenticular lodes, and (3) steeply dipping veins. At Kairagach, steeply dipping (75–80°) vein-like lodes and disseminated ore zones (sometimes flattening up to 10° at shallow levels) are typical. K–Ar and Rb–Sr dating of sericite yielded ages of 280 ± 8 Ma and 270 ± 8 Ma for pipe-like ore bodies and flat lodes plus veins at Kochbulak, respectively, while an age of 280 ± 5 Ma was obtained for the lodes at Kairagach (*Kovalenker* et al., 2004).

Ore mineralogy

The ore-forming processes at Kochbulak and Kairagach can be subdivided into pre-ore, ore, and post-ore stages. Mineralization of the pre-ore stage consists of vuggy silica with pyrophyllite, diaspore, kaolinite, and alunite, as well as quartz-carbonate-sericite-pyrite rocks. The vuggy silica is present mostly at shallow levels of the Kairagach deposit, whereas quartz-carbonate-sericite-pyrite rocks are widespread throughout the Kochbulak and Kairagach ore fields.

Three ore stages were recognized in the Kochbulak deposit by *Kovalenker* et al. (1980, 1997). Mineralization of the first stage consists of fine-grained to cryptocrystalline gray silica with variable amounts of pyrite, followed by quartz and minor dolomite and barite with native gold, tellurides, and sulfosalts (Figs. 3a, 4a). The second stage consists of banded silica, which in places occurs as a matrix cementing clasts of quartz-pyrite aggregates of the first ore stage or altered porphyries (Fig. 3a), and contains native gold, bismuthinite, and tellurides. Hydrothermal mineralization of the third stage includes white quartz with pyrite, goldfieldite, famatinite-luzonite, and minor Au and Ag tellurides (Fig. 4b), followed by fine-grained quartz with tetrahedrite, chalcopyrite, Sb- and Bi sulfosalts, Cu–Fe sulfostannates, tellurides, and sulfosalts of the lillianite series (Fig. 4c).

Fluid inclusion data (*Kovalenker* et al., 1997) showed homogenization temperatures from ~100 to 400 °C for the first ore stage, ~100 to 300 °C for the second ore stage, and ~100 to 320 °C for the third ore stage. Fluid inclusions in quartz at the beginning of each ore stage exhibited low to moderate salinity (0.5–6.5 wt.% equiv NaCl) with NaCl and KCl being the dominant salts. Fluids responsible for the formation of quartz and barite spatially associated with tellurides and sulfosalts had temperatures ~250 to 130 °C. The salinities of these fluids were 8–25 wt.% equiv NaCl, with Fe^{2+}, Mg^{2+} and Ca^{2+}, or Na^{+} and Ca^{2+} being the dominant cations in solution.

At the Kairagach deposit there are two ore stages. The first (early) ore stage consists of gray metasomatic quartz with disseminated pyrite and minor chalcopyrite, and rare sphalerite, galena, and fahlores. Native gold is interspersed as inclusions in quartz and pyrite (Fig. 3b).

The second (main) ore stage includes several assemblages that are closely related in time and are often telescoped spatially. The earliest assemblage consists of segregations of native gold in quartz-barite aggregates while the next assemblage is composed of goldfieldite and famatinite-luzonite. Later mineral assemblages include: native gold with early tellurides, native tellurium with Au, Ag, Sb, and Bi tellurides, and Cu and Fe sulfostannates (mawsonite, stannoidite, kesterite, nekrasovite, volfsonite, hemusite). A bismuth-sulfoselenide assemblage contains native bismuth, Bi-selenides, sulfoselenides, sulfotellurides, and sulfoselenotellurides, and

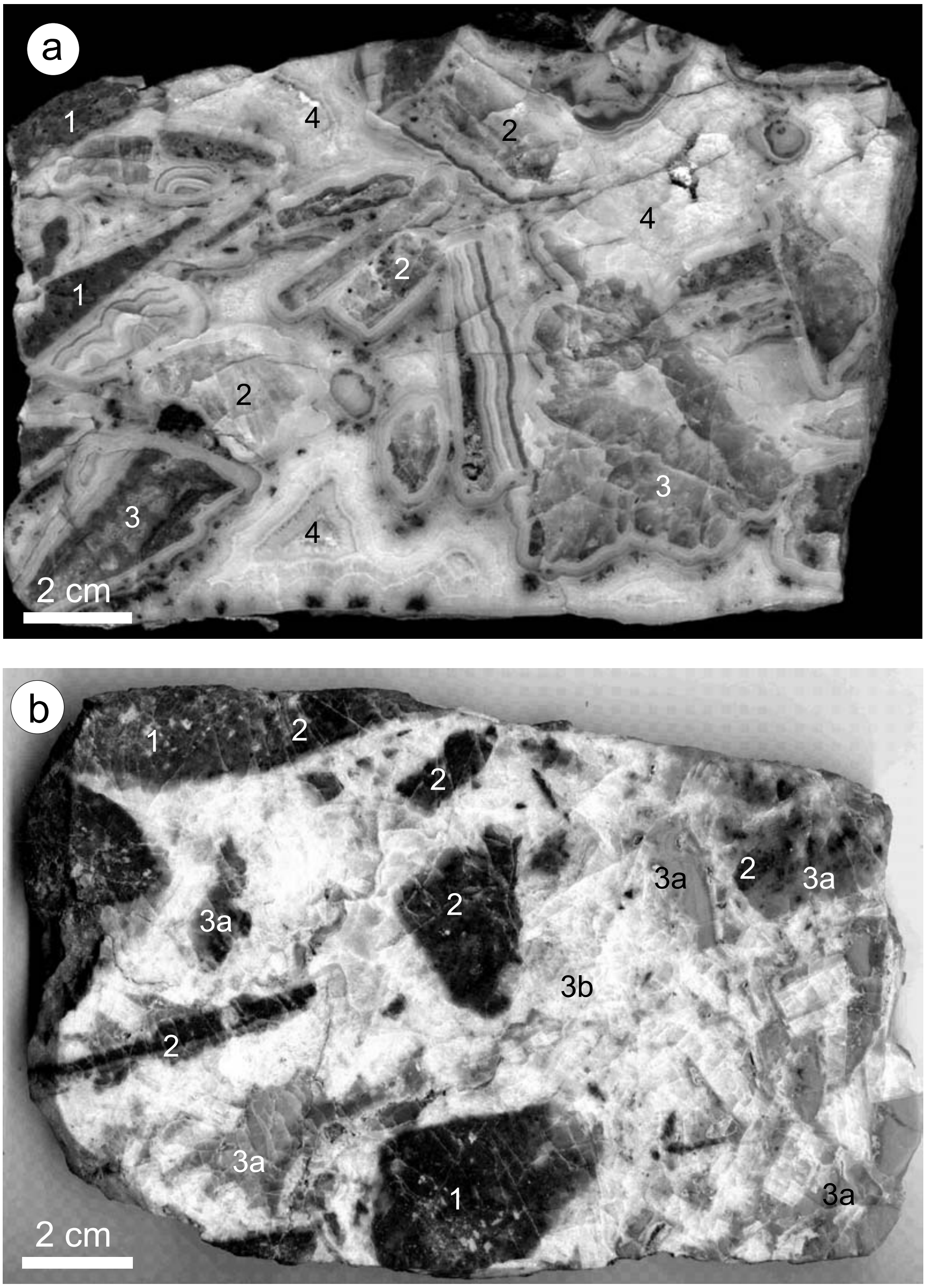

Fig. 3. Specimens showing mineral successions of the Kochbulak (a) and Kairagach (b) deposits. (a): 1. altered andesite porphyry cluster, 2. quartz of the pre ore stage, 3. quartz of the first ore stage, 4. matrix-banded quartz of the second ore stage. (b): 1. pre ore alteration – quartz-sericite-pyrite-carbonate rocks, 2. the first ore stage – vuggy silica with pyrite and disseminated native gold, 3. the second ore stage – chalcedonic silica with native gold (3a), and barite with gold–telluride–sulphosalts mineralization (3b)

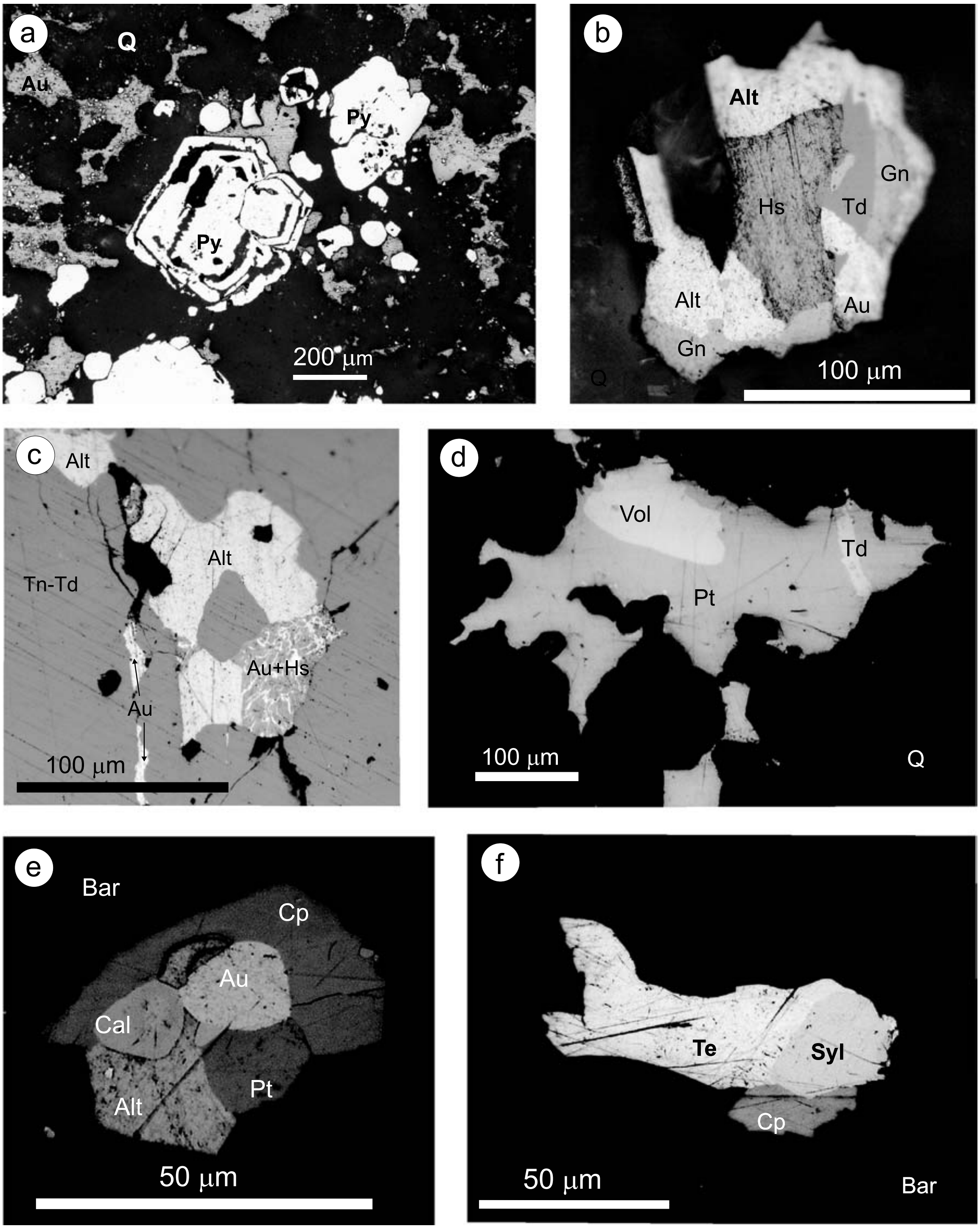

Fig. 4. Reflected light photomicrographs of mineral assemblages of Kochbulak (a–d) and Kairagach (e–f) deposits. (a) first ore stage – native Au and pyrite (Py) in quartz (Q); (b) native Au, altaite (Alt), hessite (Hs), galena (Gn), and tetrahedrite (Td) in quartz (Q) in the third ore stage; (c) native Au with hessite and altaite in tennantite–tetrahedrite (Tn–Td) in the third ore stage; (d) petzite (Pt), volynskite (Vol) and tetradymite (Td) in quartz; (e) native Au, calaverite (Cal), petzite (Pt) and chalcopyrite (Cp) in barite (Bar); (f) native Te, sylvanite (Syl), and chalcopyrite (Cp) in barite (Bar)

chalcopyrite. The Bi-sulfosalts assemblage consists of minerals of the bismuthinite-aikinite series. Near the end of the main ore stage, hessite, electrum, and chalcopyrite are common. Fahlores are intergrown with chalcopyrite to form aggregates up to several millimeters in length and contain numerous inclusions of native gold, Bi-sulfosalts, sulfostannates, tellurides, and selenides and minerals of the junoite and pavonite homologue series (*Plotinskaya* and *Kovalenker*, 1998; *Kovalenker* et al., 2003).

The main ore stage was formed at 120 to 309 °C whereas telluride-bearing barite and quartz formed at 150 to 240 °C from low to moderately saline (0.9–13.4 wt.% equiv NaCl) fluids dominated by Na^+ and K^+ (*Plotinskaya* et al., 2001; *Kovalenker* et al., 2003).

Post-ore stage mineralization for both deposits consists of quartz-carbonate-barite veinlets that crosscut minerals of the preceding stages. These veinlets also contain galena and sphalerite with rare chalcopyrite, pyrite, and tetrahedrite.

Electron microprobe analyses

Chemical compositions of ore minerals were obtained with JEOL 5900 LV SEM and LEO-1455-VP scanning electron microscopes equipped with EDX-detectors (both NHM) and with Cameca MS-46 (IGEM RAS), Camebax-Micro (TsNIGRI), Camebax SX-50 (IGEM RAS), and Cameca-SX50 (NHM) WDX electron microprobes with the following operating conditions and standards. Each instrument used an accelerating voltage of 20 kV and possessed a beam diameter of 1–2 µm. The Cameca MS-46 electron microprobe used a sample current of 15–25 nA (depending on minerals analyzed) and the analytical lines: K_α (for S, Fe, Cu, and Zn), K_β (for As); L_α (for Ag, Sb, Te, Bi, and Se). Standards used were stoichiometric FeS_2, $CuFeS_2$, NiAs, Ag_8SnS_6, and PbSe, as well as pure metallic V, Zn, Sb, Ag, Te, and Bi. The Camebax-Micro electron microprobe used a sample current of 15 nA and analytical lines: K_α (for Cu, As, S, and Se) and L_α (for other elements). Standards used were synthetic PbTe, CdSe, $CuSbS_2$, and GaAs and chemically pure Au, Ag, and Bi. The Camebax SX-50 electron microprobe used a sample current of 20 nA and analytical lines: K_α (for Cu, As, S, and Se) and L_α (for other elements). Standards used were synthetic PbTe, HgTe, FeS_2, ZnS, and GaAs and chemically pure metals.

The Cameca-SX-50 electron microprobe used a sample current 20 nA and beam diameter of 1–2 µm and up to 10–20 µm for petzite and empressite. The analytical lines measured were K_α (for Cu, S, Fe and Zn), L_α (for Te, Ag, Sb, As, and Se), M_α (for Bi, Pb, and Au). Standards used were HgTe for Te and Hg, BiTe for Bi, PbS for Pb, ZnS for S and Zn, GaAs for As, PbSe for Se, chemically pure metals for Ag, Au, Sb, Cu, and Fe.

Gold, telluride and selenide mineralogy

Telluride and selenide mineralization at Kochbulak and Kairagach consists of >30 minerals including several unknown and possible new minerals. Tellurides usually occur as small inclusions in gangue minerals (quartz at Kochbulak and in barite and rarely calcite at Kairagach) or in fahlore group minerals. They also form intergrowths with native gold and sulfides (chalcopyrite, pyrite, and galena). Native gold and tellurides are most abundant in pipe-like ore bodies at Kochbulak where gold grades reach several thousands ppm and where tellurides locally form segregations up to 10–15 cm in length.

Native gold

Native gold from both deposits has a variety of morphologies: xenomorphic, elongate, lumpy, stringer-shaped, rounded, and oval. Grains vary in size from <2 μm in the assemblage quartz + sericite in the Kairagach deposit, to 2–3 mm in telluride assemblages in the Kochbulak deposit. Native gold occurs in almost all mineral assemblages and shows marked compositional variations (Tables 1 and 2, Fig. 5a and b).

The main metal with which native gold forms an alloy is Ag (up to 46.0 wt.% in Kochbulak and up to 46.6 wt.% in Kairagach), but it also contains Hg (up to 0.9 wt.% in Kochbulak and up to 11.3 wt.% in Kairagach), and Cu (up to 2.9 wt.% in Kochbulak and 2.4 wt.% in Kairagach). Most of the gold was deposited in the assemblage quartz + sericite or in chalcedonic silica prior to the deposition of tellurides. As shown in Fig. 5a, each ore stage at Kochbulak commences with native gold of very high fineness with a subsequent increase in Ag content from early to late assemblages. A similar trend was observed for the second ore stage of native gold in the Kairagach deposit (Fig. 5b). In places, relatively high Hg contents (up to 11.4 wt.%) were identified in veinlet-like electrum within fahlore grains at Kairagach (assemblage 10 in Table 2 and Fig. 5b).

Gold and silver tellurides

Calaverite ($AuTe_2$) is one of the most common tellurides in both deposits. At Kairagach, it occurs within early assemblages of the second ore stage together with native gold of high fineness, petzite, altaite (Fig. 4d), and, in places, with tetrahedrite and tellurantimony. At Kochbulak, it is typically present in early assemblages of all three ore stages, and forms aggregates with native gold, petzite, altaite, krennerite, and galena (Fig. 4b). Calaverite contains up to 1.8 wt.% Ag, up to 0.9 wt.% Cu, and up to 3.0 wt.% Sb (Table 3).

Hessite (Ag_2Te) is also a common telluride. At Kairagach, it occurs in contact with native gold and chalcopyrite, whereas at Kochbulak it also coexists with petzite, lillianite, and tetradymite (Figs. 4b and c). As a rule, it is confined to mineral assemblages formed late in the paragenetic sequence. Stützite ($Ag_{5-x}Te_3$) occurs in the same assemblages as hessite but is much less common. Petzite (Ag_3AuTe_2) forms intergrowths with calaverite, hessite and native gold (Fig. 4e) whereas sylvanite ($AuAgTe_4$) is less common than the other precious metal tellurides but it occurs with native tellurium, empressite (AgTe), and Bi and Sb tellurides (Fig. 4f), and rarely, with other Au–Ag tellurides. At Kairagach, sylvanite contains 1.9–4.7 wt.% Cu, which occupies an intermediate position in the

Table 1. *Chemical composition of native gold and electrum from assemblages in the Kochbulak deposit (modified after* Kovalenker *et al., 1997)*

		Assemblage	n		Au wt.%	Ag wt.%	Cu wt.%	Hg wt.%	Ag at.%
First ore stage	1	Quartz ± Pyrite ± Sericite	15	range	93.40–98.25	0.46–6.40	0.04–0.49	<0.52	6.4
				mean	95.98	3.21			
	2	Calaverite ± Krennerite ± Sylvanite ± Altaite	4	range	91.77–93.61	5.52–7.62	0.04–0.10	n.d.	11.3
				mean	92.45	6.51	0.07		
	3	Altaite ± Petzite ± Coloradoite ± Tellurobismutite ± Melonite ± Tellurantimony	11	range	85.56–92.52	7.61–12.49	n.d.	n.d.	16.9
				mean	89.19	9.96			
	4	Petzite + Hessite ± Chalcopyrite	8	range	80.12–85.35	14.77–19.06	0.00–1.41	0.00–0.87	27.8
				mean	81.93	17.41	0.26		
	5	Hessite ± Petzite ± Lillianite	1		50.31	45.98	0.86	0.17	61.2
Second ore stage	6	Quartz + Sericite	9	range	94.38–99.70	0.00–5.68	0.02–0.06	0.10–0.52	3.3
				mean	97.90	1.84	0.04	0.32	
	7	Calaverite + Altaite	5	range	90.24–95.02	2.69–10.62	0.02–0.75	0.09–0.29	11.7
				mean	92.31	6.74	0.16	0.20	
	8	Altaite + Tellurobismutite ± Coloradoite ± Chalcopyrite	2	range	86.06–88.25	11.50–11.93	0.00–0.10	0.06–0.40	19.7
				mean	87.15	11.71	0.05	0.23	
	9	Bismuthinite + Tetradymite	7	range	79.88–87.63	11.40–18.87	0.06–0.64	0.05–0.15	23.9
				mean	84.88	14.71	0.26	0.11	
	10	Petzite + Hessite ± Sylvanite ± Tetradymite ± Chalcopyrite	3	range	81.07–82.61	16.45–18.25	0.19–0.36	0.11–0.33	28.1
				mean	81.74	17.64	0.18	0.19	
	11	Hessite + Chalcopyrite	3	range	75.51–77.89	20.91–25.03	0.06–0.54	0.15–0.16	35.3
				mean	75.61	22.88	0.34	0.15	

(*continued*)

Table 1 (*continued*)

		Assemblage	n		Au wt.%	Ag wt.%	Cu wt.%	Hg wt.%	Ag at.%
Third ore stage	12	Calaverite + Sylvanite ± Altaite	2	range	85.12–91.09	6.76–14.90	0.04–1.10	n.d.	17.5
				mean	88.58	10.57	0.35		
	13	Petzite ± Sylvanite ± Tetradymite	3	range	85.83–88.22	10.29–13.38	0.12–1.50	0.02–0.07	19.7
				mean	87.16	12.03	0.69	0.05	
	14	Petzite + Hessite ± Tetradymite	8	range	79.46–89.14	11.51–22.05	0.01–0.39	0.00–0.32	28.9
				mean	82.00	18.54	0.11	0.13	
	15	Hessite + Lillianite ± Petzite ± Tetradymite ± Chalcopyrite	12	range	67.50–76.82	23.43–32.28	0.05–0.27	0.00–0.21	40.6
				mean	72.26	27.29	0.12	0.12	
	16	Lillianite ± Hessite ± Chalcopyrite	12	range	55.94–64.82	35.28–43.18	0.01–2.92	0.12–0.61	53.7
				mean	60.04	39.32	1.42	0.35	

n number of analyses, *n.d.* not detected. Analyzed with Camebax-Micro (TsNIGRI) and Cameca SX50 (NHM)

Table 2. *Chemical composition of native gold from different assemblages of the second ore stage of the Kairagach deposit*

	Assemblage	n		Au wt.%	Ag wt.%	Cu wt.%	Pb wt.%	Bi wt.%	Te wt.%	Hg wt.%	Ag,at.%
1	Quartz ± Pyrite ± Sericite	28	range	87.79–99.41	0.12–10.90	0.00–0.10	0.00–0.23	0.00–0.51	0.00–0.10	0.00–0.30	2.8
			mean	97.40	1.55	0.03	0.05	0.09	0.02	0.04	
2	Quartz + Barite	8	range	87.21–97.25	0.46–9.45	0.00–0.1	0.00–0.16	0.00–1.46	0.00–0.62	0.00–0.05	8.7
			mean	93.03	4.97	0.05	0.04	0.29	0.10	0.01	
3	Altaite + Calaverite ± Petzite ± Chalcopyrite	14	range	84.04–97.01	0.39–15.35	0.00–1.15	0.00–2.18	0.00–1.55	0.00–2.70	0.00–0.30	8.9
			mean	92.24	5.17	0.23	0.30	0.21	0.23	0.05	
4	Tetradymite ± Volyn-skite ± Chalcopyrite	7	range	86.38–98.81	0.45–11.73	0.00–0.07	0.00–0.36	0.00–1.66	0.00–0.24	0.00–0.20	8.4
			mean	93.35	4.95	0.02	0.10	0.63	0.05	0.03	
5	Bismuthite-Aikinite ± Chalcopyrite	25	range	71.78–95.48	2.18–27.14	0.00–1.87	0.00–0.51	0.00–0.82	0.00–0.07	0.00–0.17	18.7
			mean	86.89	11.39	0.18	0.16	0.22	0.02	0.02	
6	Fahlore ± Chalcopyrite ± Cu–Fe-Sulfostannates	26	range	82.53–95.56	1.08–16.01	0.26–2.52	0.00–0.50	0.00–1.11	0.00–0.19	0.00–1.28	12.9
			mean	90.20	7.68	0.79	0.12	0.30	0.04	0.36	
7	Hessite ± Chalcopyrite	13	range	77.94–95.22	4.32–20.26	0.00–0.47	0.00–0.76	0.00–0.87	0.00–0.36	0.00–0.11	20.7
			mean	85.80	12.58	0.11	0.19	0.16	0.05	0.02	
8	Emplectite ± Chalcopyrite	4	range	72.00–93.13	6.41–24.32	0.04–0.34	0.00–0.15	0.00–2.02	n.d.	n.d.	19.3
			mean	86.92	11.96	0.22	0.07	0.78			
9	Chalcopyrite	12	range	67.11–82.69	16.15–29.26	0.02–1.78	0.00–0.56	0.00–0.90	0.00–1.11	0.00–0.81	30.7
			mean	78.64	19.69	0.53	0.19	0.26	0.14	0.09	
10	Fahlore	15	range	40.02–86.16	12.33–46.58	0.13–2.35	0.00–0.14	n.d	n.d.	0.00–11.26	32.7
			mean	74.50	22.13	1.20	0.06			2.08	

n number of analyses, *n.d.* not detected. Analyzed with Cameca MS-46 and Camebax SX-50 (IGEM RAS)

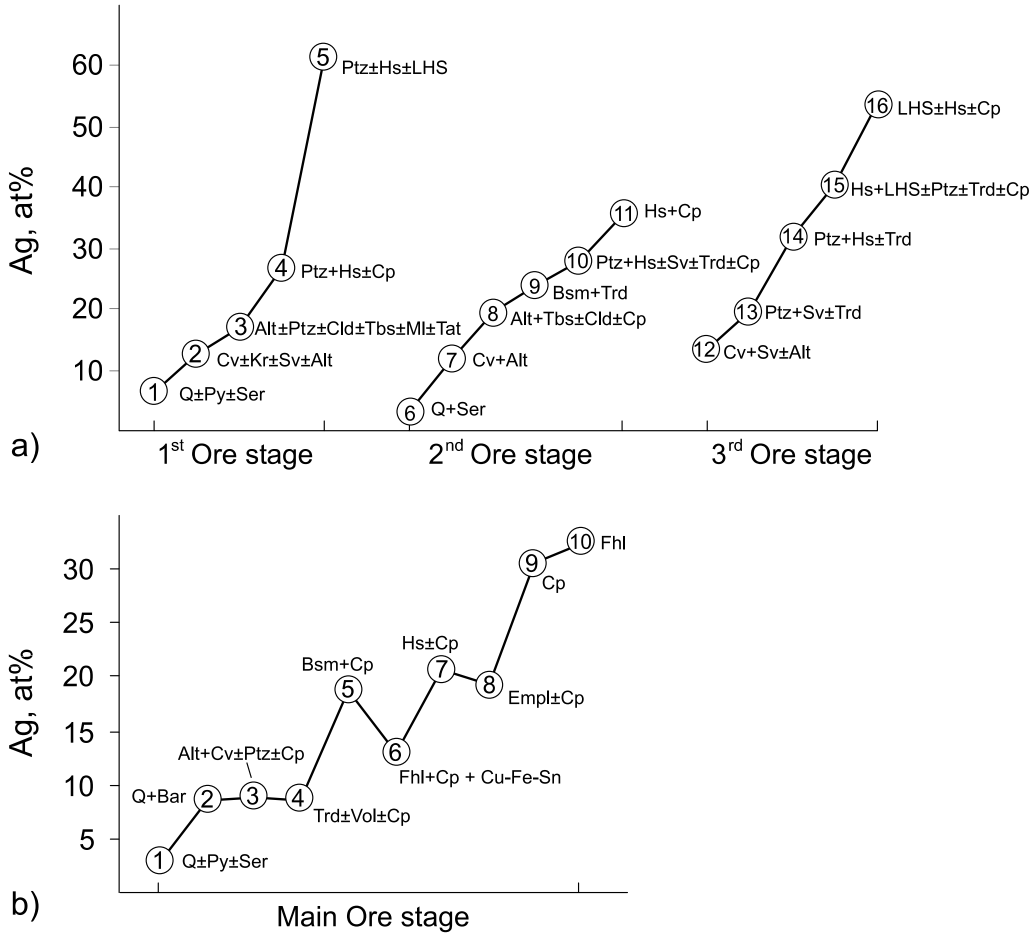

Fig. 5. Ag contents of native gold from different mineral assemblages of Kochbulak (a) and Kairagach (b) deposits. *Q* quartz; *Ser* sericite; *Alt* altaite; *Bsm* bismuthinite; *Cld* coloradoite; *Cp* chalcopyrite; *Cu–Fe–Sn* sulfostannates of Fe and Cu; *Cv* calaverite; *Empl* emplectite; *Fhl* fahlores; *Hs* hessite; *Kr* krennerite; *LHS* sulphosalts of lillianite series; *Ml* melonite; *Ptz* petzite; *Py* pyrite; *Sv* sylvanite, *Tat* tellurantimony; *Tbs* tellurbismuthite; *Te* native tellurium; *Trd* tetradymite; *Vol* volynskite

sylvanite–kostovite ($AuCuTe_4$) isomorphous series. Volynskite ($AgBiTe_2$) occurs in assemblages with Bi tellurides and petzite (Fig. 4d). Krennerite [$(Au,Ag)_2Te_4$], empressite, and kostovite are extremely rare and have been found only in the Kochbulak deposit.

Bismuth tellurides and selenides

Bismuth tellurides are intergrown with each other as well as with petzite (Fig. 4d) and native gold in early ore assemblages or they occur as decomposition products of Te- and Se- containing Bi-sulfosalts in relatively late assemblages.

Tetradymite (Bi_2Te_2S) is the most common Bi telluride and occurs with bismuth sulfosalts (bismuthinite–aikinite, junoite, and minerals of the lillianite series),

Table 3. *Representative electron microprobe analyses of tellurides and selenides from the Kochbulak and Kairagach deposits*

	Ag	Au	Cu	Pb	Fe	Hg	Bi	Sb	Te	Se	S	Total	n	Ag	Au	Cu	Pb	Fe	Hg	Bi	Sb	Te	Se	S
1	0.64	41.46	0.01	0.04	0.05	0.33	0.00	0.49	56.98	0.07	0.01	100.07	3	0.03	0.94	0.00	0.00	0.00	0.01	0.00	0.02	1.99	0.00	0.00
2	61.96	0.17	0.08	0.15	0.01	0.00	0.09	0.30	36.52	0.04	0.05	99.35	3	1.98	0.00	0.00	0.00	0.00	0.00	0.00	0.01	0.99	0.00	0.00
3	41.29	24.06	0.00	0.01	0.00	0.00	0.00	0.15	32.44	0.00	0.00	97.94	6	3.02	0.96	0.00	0.00	0.00	0.00	0.00	0.01	2.00	0.00	0.00
4	44.51	0.01	0.02	0.04	0.02	0.22	0.04	0.42	53.19	0.05	0.00	98.52	2	0.99	0.00	0.00	0.00	0.00	0.00	0.00	0.01	1.00	0.00	0.00
5*	12.96	24.74	0.00		–		0.00	0.30	63.40		0.00	101.40	6	0.97	1.01	0.00				0.00	0.02	4.00		0.00
6	7.72	25.62	2.91	0.14	0.00		0.00	0.45	63.64	0.06	0.00	100.54	6	0.57	1.04	0.37	0.01	0.00		0.00	0.03	3.98	0.01	0.00
7*	10.64	28.41	0.02		0.21		–		61.15	0.05	0.06	100.54	6	0.81	1.19	0.00		0.03			0.00	3.95	0.01	0.02
8	19.14	0.01	0.05	0.00	0.00	0.06	35.29	0.23	43.84	0.16	0.04	98.81	4	1.02	0.00	0.00	0.00	0.00	0.00	0.97	0.01	1.97	0.01	0.01
9	0.48	0.13	0.04	0.17	0.04	0.26	57.39	0.28	35.56	0.95	4.09	99.40	5	0.03	0.00	0.00	0.01	0.01	0.01	1.95	0.02	1.98	0.09	0.91
10	0.27	0.01	0.04	0.30	0.01	0.26	56.90	0.33	34.93	1.89	3.79	98.72	5	0.02	0.00	0.00	0.01	0.00	0.01	1.95	0.02	1.96	0.17	0.85
11*	0.86		0.19	13.47	0.00		38.14	0.35	45.07	0.19	0.01	98.28	7	0.09		0.03	0.73	0.00		2.06	0.03	3.98	0.03	0.00
12*	0.46		0.08		0.01		50.70	0.82	48.67	0.16	0.04	100.94	5	0.03		0.01	0.00	0.00		1.90	0.05	2.98	0.02	0.01
13	0.65	0.04	0.09	0.18	0.01		49.87	1.40	47.98	0.21	0.02	100.44	5	0.05	0.00	0.01	0.01	0.00		1.87	0.09	2.94	0.02	0.01
14	0.50	0.06	0.00	0.87	0.01	0.15	0.12	38.38	59.13	0.07	0.00	99.27	5	0.03	0.00	0.00	0.03	0.00	0.00	0.00	1.99	2.93	0.01	0.00
15	0.71	0.15	0.02	0.13	0.04		34.47	12.45	50.64	0.13	0.02	98.76	5	0.05	0.01	0.00	0.00	0.01		1.22	0.76	2.93	0.01	0.00
16	0.00	0.00	0.02	1.00	0.04		49.61	4.05	36.00	9.51	0.06	100.28	5	0.00	0.00	0.00	0.04	0.00		1.74	0.24	2.07	0.88	0.01
17*	0.29	0.37	1.39			0.71	55.92	0.44	30.58	9.12	1.75	100.57	5	0.02	0.01	0.15	0.00	0.00	0.02	1.88	0.03	1.69	0.81	0.38
18*	0.15		0.34	0.26	0.10		80.19	0.10		17.00	2.44	100.58	7	0.01	0.00	0.05	0.01	0.02		3.83	0.01	0.00	2.15	0.76
19	0.29	0.00	1.44	1.17	0.18	0.00	85.68	0.03	0.05	7.06	7.13	103.04	2	0.01	0.00	0.06	0.01	0.01	0.00	1.08	0.00	0.00	0.24	0.59
20	0.22	0.06	0.00	61.80	0.00	0.00	0.18	0.25	36.88	0.49	0.07	99.94	2	0.01	0.00	0.00	0.99	0.00	0.00	0.00	0.01	0.96	0.02	0.01
21*			2.31	69.63	1.45		0.26			23.39	3.63	100.67	2			0.09	0.83	0.06		0.00		0.00	0.73	0.28
22	0.00	0.06	0.71	0.00	16.89	0.39	0.07	0.54	81.22	0.00	0.02	99.90	3	0.00	0.00	0.04	0.00	0.95	0.01	0.00	0.01	1.99	0.00	0.00
23	0.14	0.06	0.00	0.04	0.05	59.45	0.00	0.36	38.12	0.01	0.00	98.22	2	0.00	0.00	0.00	0.00	0.00	0.99	0.00	0.01	0.99	0.00	0.00
24	0.09	0.03	0.07	0.01	0.01		0.00	0.70	98.62	0.15	0.01	99.69												
25*	0.05		0.01	0.08	0.01			0.39	90.31	10.25	0.09	101.19												

Note: * Cameca MS 46, other analyses – Cameca SX 50; *n* number of atoms; *1* calaverite; *2* hessite; *3* petzite; *4* empressite; *5* sylvanite; *6* Cu-sylvanite, *7* krennerite; *8* volynskite; *9* tetradymite; *10* Se-tetradymite; *11* rucklidgeite; *12* phase Bi_2Te_3; *13* tellurobismuthite; *14* tellurantimony; *15* $(Bi,Sb)_2Te_3$; *16* $(Bi,Sb)_2$,Te_2Se; *17* kawazulite; *18* laitakariite; *19* Bi (S,Se); *20* altaite; *21* clausthalite; *22* frohbergite, *23* coloradoite; *24*, *25* native Te

Au–Ag tellurides, and native gold. Tetradymite contains up to 4 wt.% Se. Rare rucklidgeite ($PbBi_2Te_4$) and tellurobismuthite (Bi_2Te_3) occur with tetradymite in both the Kochbulak and Kairagach deposits. Joseite [$Bi_3Te(Se,S)$] and tsumoite (Bi_3Te_2Se) occur at Kochbulak whereas sulfotsumoite [$Bi_3Te_2(S,Se)$] occurs at Kairagach. Kawazulite (Bi_2Te_2Se) and Sb-kawazulite [$(Bi,Sb)_2Te_2Se$] were observed at Kairagach in intergrowths with native tellurium. An unnamed mineral with the formula [$(Bi,Sb)_2Te_3$], occurs within empressite, sylvanite and tetradymite at the Kochbulak deposit. It is presumably transitional within the tellurobismuthite (Bi_2Te_3)-telluroantimony (Sb_2Te_3) isomorphic series. Other unnamed phases with the following formulas: $AgBi_3Te_5$, $Ag_3Bi_5Te_9$, and $Pb_2Bi_6Te_{11}$ were reported at Kochbulak by *Kovalenker* et al. (1980, 1997).

Bismuth selenides and sulfoselenides were observed only in ores from Kairagach. These minerals are guanajuatite (Bi_2Se_3), laitakarite [$Bi_4(S,Se)_3$], nevskite [$Bi(Se,S)$] and unnamed phases with formulae $CuBi_3(S,Se)_5$ and $Cu_2Bi_{15}(S,Se)_{11}$. The following unnamed phases Bi_2SeS, Bi_3TeSe and Bi_3Te_2SeS were also reported by *Spiridonov* and *Badalov* (1983).

Lead tellurides and selenides

Altaite (PbTe) is as abundant as calaverite and hessite and occurs in both deposits in an assemblage with calaverite and native gold. Clausthalite (PbSe), as well as Se-rich galena [Pb(S,Se)] with S contents from 2.4 to 11.6 wt.% occurs at the Kairagach deposit in assemblages with famatinite-luzonite, Te-tetrahedrite, chalcopyrite, and Cu–Fe-sulfostannates. At Kochbulak, small ($<5\ \mu m$) single grains of Se-rich galena from the first ore stage were identified by EDX in an assemblage with chalcopyrite, tetrahedrite, famatinite, and goldfieldite.

Other tellurides and selenides

Coloradoite (HgTe) and frohbergite ($FeTe_2$) occur at both deposits but are relatively rare and spatially associated with the same minerals as altaite. Telluroantimony (Sb_2Te_3) occurs in both deposits in assemblages with calaverite, native tellurium, and Sb-kawazulite. Melonite ($NiTe_2$) occurs with altaite, petzite, and coloradoite only within the first ore stage at the Kochbulak deposit.

Cu tellurides vulcanite, (CuTe), rickardite (Cu_7Te_5) and weissite (Cu_5Te_3) were found in the Kochbulak deposit as intergrowths with covellite, chalcocite, and tellurite (TeO_2) and are presumably of supergene origin.

Native tellurium

Native tellurium was found at both deposits. At Kairagach, it occurs as intergrowths with tellurantimony, calaverite, Cu-sylvanite, clausthalite, and Sb-kawazulite where, in places, it is overgrown by chalcopyrite. At shallow levels, native Te contains up to 10.3 wt.% Se and up to 0.5 wt.% Sb whereas at deep levels it contains up to 0.2 wt.% Se and up to 0.7 wt.% Sb. At the Kochbulak deposit native Te occurs mostly within the first ore stage in pipe-like ore bodies where it forms crystals up to 2 cm in size and as intergrowths with empressite, sylvanite, altaite, and an unnamed phase [$(Bi,Sb)_2Te_3$] within the third ore stage.

Discussion

Tellurides within three ore stages at the Kochbulak deposit and the main ore stage at Kairagach precipitated in similar paragenetic sequences that can be generalized as follows: calaverite + native Te, altaite + calaverite + native gold, petzite + Bi-tellurides + native gold, and hessite + native gold. The observed trend of assemblages in the system Au–Ag–Te is native Au + calaverite, followed by native Au + petzite ± hessite and, finally, native Au + hessite ± petzite. The Ag content of native gold increases from early to late in the paragenetic sequence corresponding with the Ag content in tellurides.

As shown by *Zhang* and *Spry* (1994), the change in dominance of calaverite to hessite in the precious metal assemblage (trend 1-2-3 on Fig. 6) can be caused by an increase in the activity of Ag in solution, by an increase in pH (trend 1 on Fig. 7),

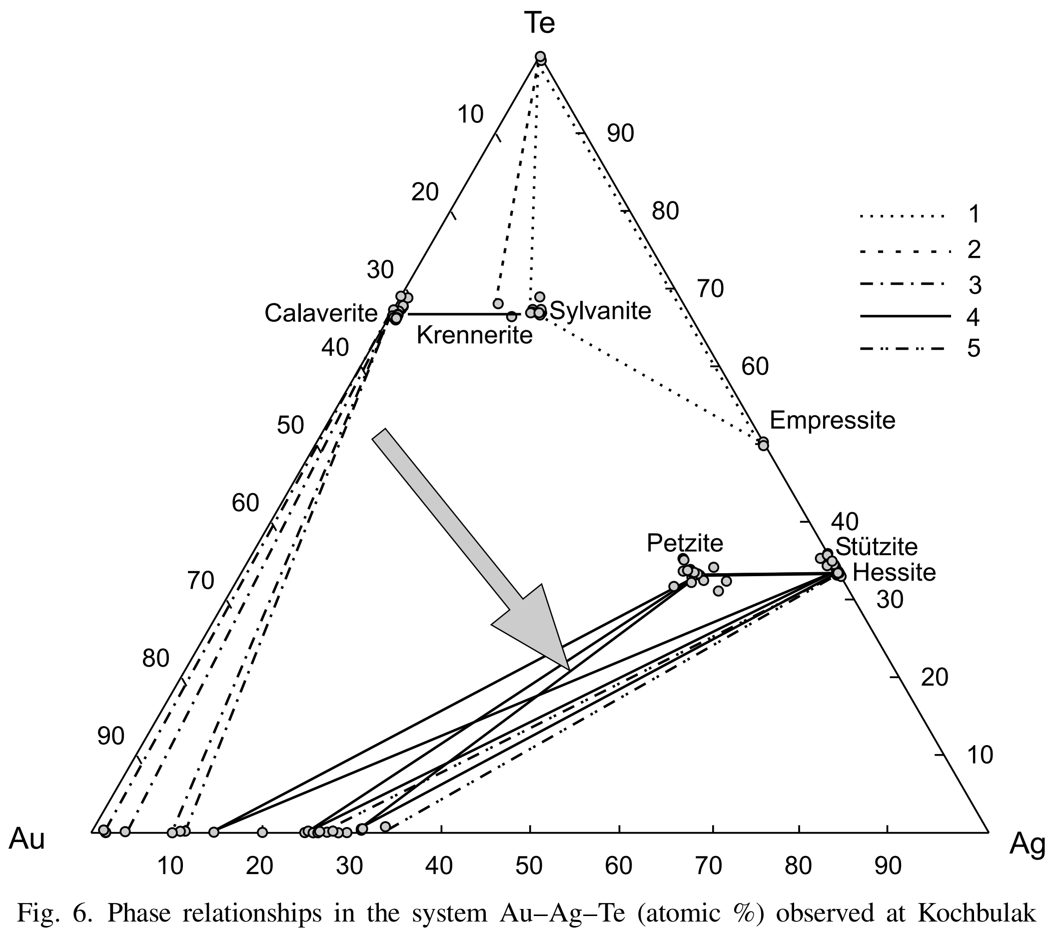

Fig. 6. Phase relationships in the system Au–Ag–Te (atomic %) observed at Kochbulak and Kairagach deposits. Mineral assemblages: (1) native tellurium ± empressite ± sylvanite; (2) native tellurium + krennerite; (3) calaverite + native gold; (4) hessite + petzite + native gold, (5) hessite + native gold. Arrow shows the general temporal trend for both deposits

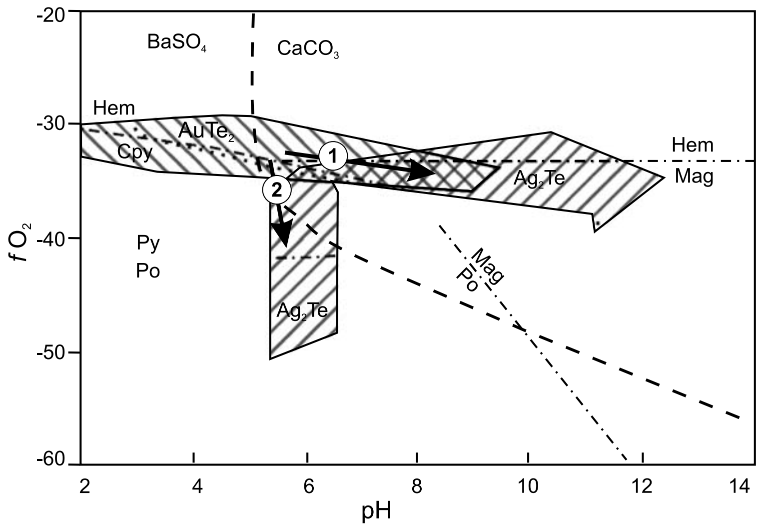

Fig. 7. Log fO_2 versus pH diagram for the stabilities of calaverite and hessite (hatched areas), barite (dotted lines), calcite (dashed lines), and for minerals of the Fe–S–O system (dashed-dotted lines) for the following conditions: $\Sigma Au = 1$ ppb, $\Sigma Ag = 1$ ppb, $\Sigma Te = 1$ ppb, and $\Sigma S = 0.01$ m. Arrows show general temporal trends for Kochbulak (1) and for Kairagach (2). Sources of data are listed in text

or by a decrease in fO_2 (trend 2 on Fig. 7). All three processes may have taken place as tellurides formed at Kochbulak and Kairagach. At the same time, an abundance of barite and the presence of calcite within the main ore stage of Kairagach suggests that fO_2 was maintained at a relatively high level (>-35 log fO_2 units for 250 °C). Thus the evolution of telluride assemblages at Kairagach was caused by an increase in pH (trend 2 on Fig. 7 was dominant). Barite and calcite are rare in ore assemblages at Kochbulak, whereas sulfides (pyrite and chalcopyrite) are more abundant than at Kairagach and suggests that a decline in log fO_2 to -40 could have been the main factor in the changing the dominance of calaverite to hessite as the main precious metal telluride (i.e. trend 1 on Fig. 7 was dominant within each ore stage).

According to the experimental studies of *Cabri* (1965), the assemblage native Te + sylvanite at both deposits and the assemblage native Te + krennerite at Kochbulak, suggest that they formed below 335 °C. Temperature estimates using the assemblage native Te + sylvanite + empressite cannot be made since it was not reported in the experimental studies of *Pellini* (1915), *Markham* (1960), *Cabri* (1965), and *Legendre* et al. (1980). However, *Cabri* (1965) reported that the assemblage native Te + sylvanite + stützite is stable at 290 °C, which is in good agreement with the fluid inclusion data.

Thermodynamic data for sulfides and tellurides by *Barton* and *Skinner* (1979) and *Afifi* et al. (1988) were used to calculate phase boundaries in Fig. 8. At the beginning of telluride deposition at approximately 250 °C, log fS_2 (-14.6 to -8.6) was controlled by the stability of pyrite and chalcopyrite. *log* fTe_2 for the formation of native Te, calaverite and tellurantimony was >-7.8 (area 1 in Fig. 8a) and decreased to a minimum of approximately -11.5 log units during the deposition

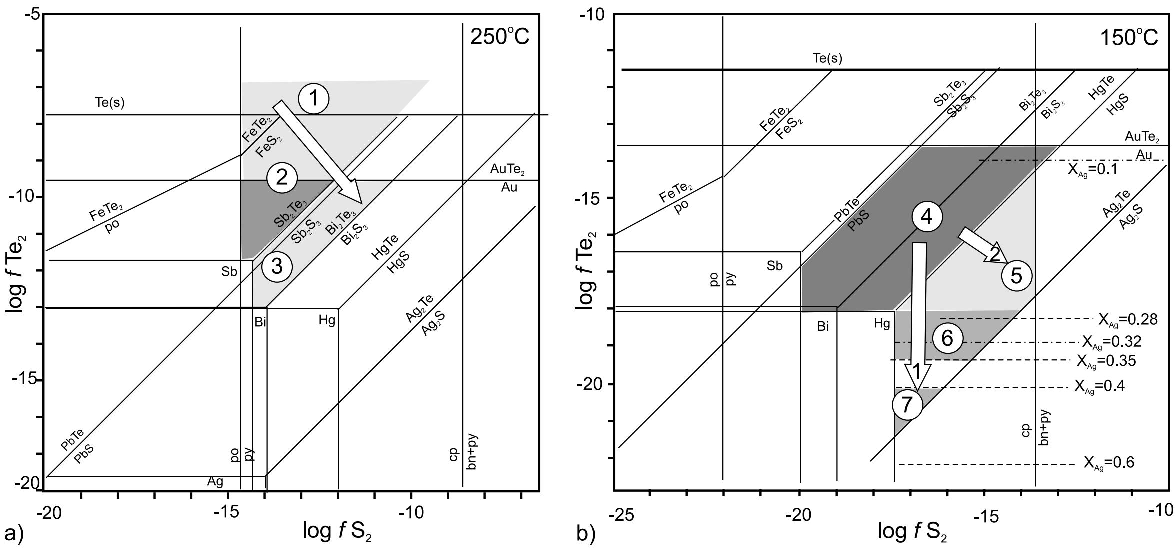

Fig. 8. Log fTe$_2$ versus log fS$_2$ diagrams calculated for 250 °C (a) and 150 °C (b). 1. native Te + calaverite + tellurantimony, 2. native gold + altaite and native gold + calaverite, 3. native gold + Bi tellurides, 4. native gold + Bi sulfosalts, 5–7. hessite + native gold with: 5. 10 to 32 at.% of Ag (Kairagach), 6. 28 to 35 at.% of Ag and 7. 40 to 60 at.% of Ag (Kochbulak). Arrows show general trends for Kochbulak (1) and Kairagach (2). Sources of data are listed in text

of native gold + altaite + calaverite (area 2 on Fig. 8a) and further to a minimum of −13 where the assemblage native gold + tellurobismuthite was stable.

As the temperature decreased to 150 °C, coexisting pyrite and chalcopyrite are stable between log fS$_2$ = −22.0 and −13.6 (Fig. 8b). Since they coexist with native gold, galena and tellurobismuthite this suggests that log fTe$_2$ was constrained to between −18.0 and −13.6 (area 4 on Fig. 8b).

Later-formed assemblages contain native gold coexisting with hessite. Using the thermodynamic data of *Afifi* et al. (1988) and assuming that the Ag content was buffered only by fTe$_2$ allows fTe$_2$ to be determined. For native gold associated with hessite from the Kairagach deposit, Ag contents range from 10 to 28 at.% (mean 20.7 at.%), which corresponds to values of log fTe$_2$ that range from −18.9 to −11.6 (area 5 on Fig. 7a). At Kochbulak, the Ag content of native gold ranges from 28 to 35 at.% in the assemblage native gold + hessite + chalcopyrite and from 40.6 to 61.2 at.% for the assemblage native gold + hessite + lillianite. Values of logTe$_2$ range from −19.3 to 18.2, and from −22.5 to −20.1 for these assemblages, respectively. Thus, at Kochbulak the deposition of native gold and Ag tellurides was accompanied by a drop in fTe$_2$ of five orders of magnitude whereas fS$_2$ likely remained constant (trend 1 on Fig. 7a). At the Kairagach deposit, fTe$_2$ could have been constant or decreased slightly as fS$_2$ increased (trend 2 on Fig. 8a). In general, paragenetic sequence of telluride assemblages during each ore stage at both. Kochbulak and Kairagach was the result of a decrease in temperature and log fTe$_2$.

At Kairagach, selenides and sulfoselenides of Bi and Pb are common, in contrast to the Kochbulak deposit, where only Bi and Pb telluroselenides and sulfotelluriselenides were formed. Despite the absence of thermodynamic data for some

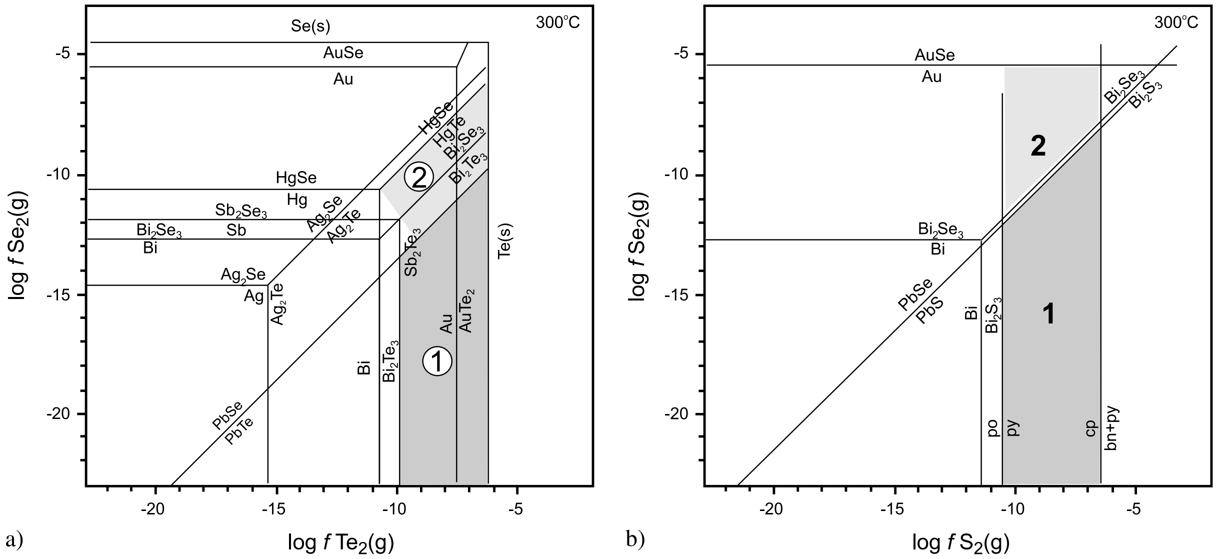

Fig. 9. Log $f\mathrm{Se}_2$ versus log $f\mathrm{Te}_2$ (a) and versus log $f\mathrm{S}_2$ (b) diagrams calculated for 300 °C. Shaded areas show the stability fields of selenides, tellurides, and sulfides at Kochbulak (1) and Kairagach (2) deposits. Sources of data are listed in text

minerals in the systems Bi–Te–Se and Bi–S–Te, the ore forming conditions can be estimated from the stability fields of guanajuatite (Bi_2Se_3) and clausthalite (PbSe) and data from *Barton* and *Skinner* (1979) and *Simon* and *Essene* (1996) (Fig. 9a and b). Values of log $f\mathrm{Se}_2 = -14.0$ to -6.5 and log $f\mathrm{Te}_2 = -11.0$ to -6.2 are obtained for the Kairagach deposit at 300 °C based on the presence of guanajuatite, clausthalite and hessite (rather than naumannite). At Kochbulak, the value of log $f\mathrm{Se}_2$ was < -8.5.

The values of $f\mathrm{S}_2$, $f\mathrm{Te}_2$, and $f\mathrm{Se}_2$ may be reflecting multiple inputs of magmatic components into the Kochbulak ore-forming system while a magmatic contribution to the Kairagach ore-forming system is less apparent. The precipitation of sulfides, tellurides, and selenides were associated with decreasing $f\mathrm{S}_2$ and $f\mathrm{Te}_2$ and increasing $f\mathrm{Se}_2$ conditions.

The deposition of abundant native gold of high fineness preceded telluride deposition in both deposits. Native gold has higher Ag contents where spatially associated with tellurides, as well as with lillianite at Kochbulak or fahlores and chalcopyrite at Kairagach. As noted by *Afifi* et al. (1988), in most epithermal deposits native gold usually precipitates either with or follows the deposition of tellurides. This has been observed at, for example, Golden Sunlight, Montana (*Porter* and *Ripley*, 1985), and Emperor, Fiji (*Pals* and *Spry*, 2003). However, in some high sulfidation deposits (e.g., Elshitsa and Radka deposits, Bulgaria, *Bogdanov* et al., 1997), native gold precipitated in the early quartz-pyrite stage, which is similar to that observed in the Kochbulak and Kairagach deposits. The most plausible explanation for this observation is that at the beginning of each stage of hydrothermal activity the initial $f\mathrm{S}_2/f\mathrm{Te}_2$ ratio was too high and allowed only sulfides and native gold to be deposited with the residual fluid being enriched in Te.

Conclusions

1. Tellurides at Kochbulak are more abundant and variable than at Kairagach but they occur in similar assemblages and three ore stages. The generalized telluride-bearing sequence is: 1. altaite + Au tellurides + native Te, 2. calaverite + native gold, 3. Bi tellurides + Au–Ag tellurides + native gold, followed by 4. Ag tellurides + native gold.
2. The Ag content of tellurides and native gold increases from early to late in the paragenetic sequence, which corresponds to a decrease in temperature and fO_2, and a concomitant increase in pH.
3. Values of log fTe_2 ranged from −13.0 to −7.8 at the beginning of telluride deposition (around 250 °C) and decreased to <−20 as the temperature declined.
4. The main difference in telluride and selenide assemblages between the two deposits is the presence of selenides and sulfoselenides of Bi and Pb at the Kairagach deposit which was, in part, caused by higher fSe_2 conditions compared to those observed at Kochbulak.

Acknowledgements

The authors would like to thank *A. Tsepin, V. Malov, N. Troneva* (IGEM RAS, Moscow), *S. M. Sandomirskaya* (TsNIGRI), *T. Williams, J. Spratt* and *A. Kearsley* (Natural History Museum, London) for the electron microprobe analyses. OP is thankful to *V. L. Rusinov* and *A. V. Zotov* (IGEM RAS) for their assistance and advice with thermodynamic calculations. This paper was greatly improved by the reviews of *P. Spry* and *E. Ronacher.*

This study was supported by the Natural History Museum, London through a CERCAMS project, by the Russian Foundation for Basic Research (project Nr 04-05-64407), and by the Russian Science Support Foundation. The research is a contribution to IGCP projects #473 and #486.

References

Afifi AM, Kelly WC, Essene EJ (1988) Phase relations among tellurides, sulfides, and oxides: I. Thermochemical data and calculated equilibria; II. Applications to telluride-bearing ore deposits. Econ Geol 83: 377–394 and 395–404

Badalov AS, Spiridonov EM (1983) Fahlores and native gold of the Kairagach mineralization (Eastern Uzbekistan) (in Russian). Uzb Geol Zh 2: 74–78

Badalov AS, Spiridonov EM, Heinke VP, Pavshukov VV (1984) Minerals-native elements and tellurides of the Kairagach volcanic-hosted mineralization (Uzbek Soviet Socialist Republic) (in Russian). Zap Uzb Otd Vses Min O-va 37: 64–67

Barton PB Jr, Skinner BJ (1979) Sulfide mineral stabilities. In: *Barnes HL* (ed) Geochemistry of hydrothermal ore deposits. Wiley Interscience, New York, pp 278–403

Bogdanov K, Tsonev D, Kuzmanov K (1997) Mineralogy of gold in the Elshitsa massive sulphide deposit, Sredna Gora zone, Bulgaria. Mineral Deposita 32: 219–229

Bonham HF Jr (1986) Models for volcanic-hosted epithermal precious metal deposits: a review. Int Volcanol Congress Symp 5. Proceedings, Hamilton, New Zealand, pp 13–17

Cabri LJ (1965) Phase relations in the Au–Ag–Te system and their mineralogical significance. Econ Geol 60: 1569–1606

Dalimov TN, Ganiev IN (1994) Zoning of magmatism in the Chatcal-Kurama region (Devonian, Middle Carbon) (in Russian) Uzb Geol Zh 3: 28–34

Genkin AD, Kovalenker VA, Safonov YG (1980) Characteristics of the ore textures and formation mechanism of pipe-like ore bodies of the Kochbulak deposit, Methods of investigation of ore-forming sulfides and their parageneses (in Russian). Moscow: Nauka 127–139

Heald P, Foley NK, Hayba DO (1987) Comparative anatomy of volcanic-hosted epithermal deposits: acid–sulfate and adularia-sericite types. Econ Geol 82: 1–26

Henley RW (1991) Epithermal gold deposits in volcanic terranes. In: *Foster RP* (ed) Gold metallogeny and exploration. Blackie, Glasgow, pp 133–164

Islamov F, Kremenetsky A, Minzer E, Koneev R (1999) The Kochbulak–Kairagach ore field. In: *Shayakubov TSh, Islamov F, Kremenetsky A, Seltmann R* (eds) Au, Ag, and Cu deposits of Uzbekistan. Excursion Guidebook, Potsdam GFZ, pp 91–106

Koneev RI, Gertman YL (1997) Microparageneses of gold in gold-ore formations of Eastern Uzbekistan. Osnovnye problemy v uchenii o magmatogennykh rudnykh mestorozhdeniyakh (Principle problems in the science on magmatic ore deposits). Moscow: Inst Geol Rudn Mest Ross Akad Nauk: 142–143 (in Russian)

Kovalenker VA, Chernyshev IV, Plotinskaya OY, Prokof'ev VY (2004) Ore mineralogy, fluid inclusions, age and isotopic characteristic of the late-Paleozoic high-sulfidation epithermal gold-telluride deposits: Kurama Mountains, Middle Tien Shan. In: *Cook J, Ciobanu CL* (eds) Au–Ag-telluride Deposits of the Golden Quadrilateral, South Apuseni Mts., Romania, Guidebook of the International Field Workshop of IGCP project 486, IAGOD Guidebook Series,: 12: 239–241

Kovalenker VA, Heinke VP (1984) A new Cu–Sn–Bi–Se type of mineralization in the Kurama subzone of the Central Tien Shan (in Russian). Izv Akad Nauk SSSR, Ser Geol 5: 91–104

Kovalenker VA, Naumov VB, Prokof'ev VYu (1980) Mineralogical and geochemical regularities and P–T parameters of the origin of productive mineral assemblages of the Kochbulak ore field (in Russian). Geol Ore Dep 1: 38–52

Kovalenker VA, Plotinskaya OY, Prokof'ev VY, Gertman YL, Koneev RI, Pomortsev VV (2003) Mineralogy, geochemistry, and genesis of gold–sulfide–selenide–telluride ores from the Kairagach deposit (Uzbekistan). Geol Ore Dep 45: 171–200

Kovalenker VA, Safonov YG, Naumov VB, Rusinov VL (1997) The Kochbulak epithermal gold–telluride deposit (Uzbekistan). Geol Ore Dep 39: 127–152

Kovalenker VA, Troneva NV, Dobronichenko VV (1980) Characteristics of main ore minerals from pipe-like ore bodies of the Kochbulak deposit (in Russian). In: *Distler VV* (ed) Methods of investigation of ore-forming sulfides and their parageneses Moscow: Nauka: 140–164

Kovalenker VA, Troneva NV, Kuz'mina OV, Vyal'sov LN, Goloshchukov PM (1979) The first finding of kostovite in the Soviet Union (in Russian). Dokl Akad Nauk SSSR 247: 564–569

Legendre B, Souleau C, Chhay H (1980) The ternary system Au–Ag–Te. Bull Soc Chim France 5–6: 197–204

Markham NL (1960) Synthetic and natural phases in the system Au–Ag–Te. Econ Geol 55: 1148–1178

Pals DW, Spry PG (2003) Telluride mineralogy of the low sulfidation epithermal Emperor gold deposit, Vatukoula, Fiji. Mineral Petrol 79: 285–307

Pellini G (1915) Telluriri di argento e oro. Gaz Chim Ital 45: 469–484

Plotinskaya OY, Kovalenker VA (1998) The Kairagach epithermal gold–telluride deposit: mineralogical–geochemical zonation. Tez Dokl Nauch Konf "Zolotorudnye mestorozhdeniya Uzbekistana:geologiya i promyshlennye tipy" (Proc. Conf "Gold-ore deposits of Uzbekistan: geology and commercial types"). Tashkent, IMR, pp 57–60 (in Russian)

Plotinskaya OY, Kovalenker VA, Prokof'ev VY, Groznova EO, Nosik LP (2001) Formation conditions of ores in the Kairagach epithermal gold–telluride deposit (Uzbekistan): fluid inclusions and stable isotopes. In: *Melnikov FP*, *Poliansky EV* (eds) Trudy X Mezhdunarodnoi konferentsii po termobarogeokhimii (Proc. X Int Conf on Thermobarochemistry) Aleksandrov: VNIISIMS, pp 158–179 (in Russian)

Porter EW, Ripley E (1985) Petrologic and stable isotope study of the gold-bearing breccia pipe at the Golden Sunlight deposit, Montana. Econ Geol 80: 1689–1706

Simon G, Essene EJ (1996) Phase relations among selenides, sulfides, tellurides, and oxides: I. Thermodynamic properties and calculated equilibria. Econ Geol 91: 1183–1208

Spiridonov EM, Badalov AS (1983) New bismuth sulfoselenotellurides and sulfoselenides from the Kairagach volcanic deposit (Eastern Uzbekistan) (in Russian). Uzb Geol Zh 6: 82–84

White NC, Hedenquist JW (1990) Epithermal environments and styles of mineralization: variations and their causes, and guidelines for exploration. J Geochem Explor 36: 445–474

Zhang X, Spry PG (1994) Calculated stability of aqueous tellurium species, calaverite and hessite at elevated temperature. Econ Geol 89: 1152–1166

Zonenshain LP, Kuzmin MI, Natapov LM (1990) Geology of the USSR: A plate tectonic synthesis. AGU Geodynam Ser Monogr 21, 240 p

Authors' addresses: *O. Plotinskaya* (corresponding author; e-mail: plotin@igem.ru, olgaplotin@yahoo.co.uk) and *V. A. Kovalenker*, Institute of Geology of Ore Deposits, Petrography, Mineralogy, and Geochemistry, Russian Academy of Sciences (IGEM RAS), Staromonetny per. 35, 119017 Moscow, Russia; *R. Seltmann* and *C. J. Stanley*, CERCAMS, Department of Mineralogy, Natural History Museum (NHM), Cromwell Road, London SW7 5BD, United Kingdom